

**Simulation of Solar Photovoltaic Power
Station**

A Thesis presented to the Faculty of the Graduate
School University of Missouri-Columbia

In Partial Fulfillment
of the Requirements for the Degree

Master of Science

by

XUQIANG LI

Dr. Thomas G. Engel, Thesis Supervisor

May 2018

The undersigned, appointed by the Dean of the Graduate School, have examined the thesis entitled

Simulation of Solar Photovoltaic Power Station

Presented by Xuqiang Li

A candidate for the degree of Master of Science

And hereby certify that in their opinion it is worthy of acceptance.

Professor Thomas G. Engel

Professor Mark A. Prelas

Professor Lin. Yuyi

ACKNOWLEDGEMENTS

This research wouldn't be possible without guidance from my faculty advisor Dr. Thomas G. Engel. The support he provided was invaluable when I was blocked by problems and could not go any further. His door was always open for me when I needed.

Also, I would like to thank my friends and my family who are from other majors for providing invaluable knowledge which has enriched my life in so many ways.

TABLE OF CONTENTS

ACKNOWLEDGEMENTS.....	ii
LIST OF FIGURES	v
LIST OF TABLES	vii
ABSTRACT.....	viii
CHAPTER 1 BACKGROUND	1
CHAPTER 2 INTRODUCTION.....	4
2.1 System classification.....	4
2.2 System equipment.....	5
2.2.1 PV Array.....	6
2.2.2 Controlling Device.....	7
2.2.3 Boost Converter.....	9
2.2.4 DC-AC Inverter	12
2.2.5 Grid	16
CHAPTER 3 MODELING.....	17
3.1 Matlab Simulink.....	17
3.2 PV Array	18
3.2.1 Light Generated Current	22
3.2.2 Controlled Current Source.....	24
3.3 MPPT Controller & Boost Converter.....	25
3.4 VSC.....	27
3.4.1 PLL.....	28
3.4.2 Outer Active-Reactive Power and Voltage Loop.....	31
3.4.3 Inner Current Loop.....	33
3.4.4 Modeling	35
3.5 Grid	36

3.5.1 Measurements Component.....	36
3.5.2 Distributed Parameter Line	37
3.5.3 RLC Load Components.....	38
3.5.4 Three-phase Transformer Components	39
 CHAPTER 4 RESULT	 41
4.1 The Performance of PV Array	41
4.2 The Performance of Boost Converter	43
4.3 The Performance of VSC Inverter	44
4.4 Efficiency	45
 CHAPTER 5 SUMMARY & CONCLUSION	 46
5.1 Overview of the Project	46
5.2 Improve Power Generation Efficiency	47
 REFERENCES	 50

LIST OF FIGURES

Figure 1.1 Pie chart of 2014 US net generation by energy source	1
Figure 2.1 PV power system.....	5
Figure 2.2 The principle of solar cells.....	7
Figure 2.3 Stand-alone photovoltaic system with MPPT.....	8
Figure 2.4 The main circuit of boost converter	10
Figure 2.5 Boost converter working condition analysis	11
Figure 2.6 Three-phase voltage bridge inverter circuit	12
Figure 2.7 Three-phase voltage bridge inverter operating waveform.....	14
Figure 2.8 The main circuit design of SPWM inverter	14
Figure 3.1 Equivalent circuit of photovoltaic cell	19
Figure 3.2 Simulation model of PV cell	22
Figure 3.3 Simulation model of light generated current	23
Figure 3.4 The waveform of temperature and solar irradiance and the resulting photocurrent	23
Figure 3.5 Simulation model of controlled current source	24
Figure 3.6 Simulation model of using INC algorithm to build PWM	25
Figure 3.7 Simulation model of general boost converter with MPPT	26
Figure 3.8 The general design model of VSC.....	27
Figure 3.9 Phase-locked loop.....	28
Figure 3.10(a) d-axis active power regulation	31
Figure 3.10(b) q-axis reactive power regulation	31
Figure 3.11 Constant DC voltage controlled converter	32
Figure 3.12 The inner current decoupling controller.....	35
Figure 3.13 The simulation model of VSC inverter.....	35
Figure 3.14 The simulation model of Grid	36

Figure 3.15 The 3-phase VI measurement component.....	37
Figure 3.16 The 3-phase distributed parameter line component.....	37
Figure 3.17 The 3-phase RLC load component.....	38
Figure 3.18 The 3-phase transformer component.....	39
Figure 4.1 The voltage and current output of PV array.....	41
Figure 4.2 The characteristics of I-V and P-V at different temperature	42
Figure 4.3 The change of voltage after using boost converter with MPPT	43
Figure 4.4 The voltage waveform after using VSC inverter	44
Figure 4.5 The voltage waveform of grid.....	44

LIST OF TABLES

Table 3.1 The parameter setting of 3-phase distributed parameter line component.....	38
Table 3.2 The parameter setting of 3-phase RLC load component.....	39
Table 3.3 The parameter setting of 3-phase transformer component	40
Table 4.1 The performance of PV array.....	42
Table 5.1 The efficiency of PV station around the world.....	47

Simulation of solar photovoltaic power station
Xuqiang Li

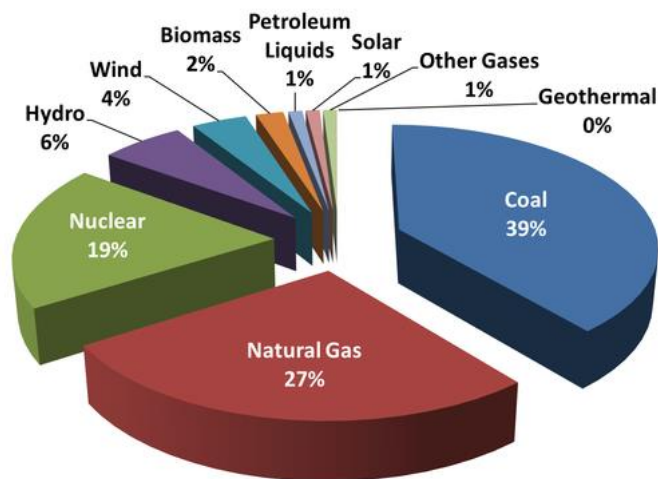
Dr. Thomas G. Engel, Thesis Supervisor

ABSTRACT

It is predicted that in the 21st century, solar photovoltaic power generation will occupy an important seat of world energy consumption, and will replace some conventional energy. Solar photovoltaic power station is a kind of power stations which use solar cell array to convert solar radiation into electricity. The system is mainly composed of solar cell array, system controller, battery, DC / AC inverter and other components. This article will mainly introduce the principle and equipment of photovoltaic power generation system and lay the foundation for the computer simulation afterwards.

Chapter 1 Background

With the continuous development of the global economy, the demand for traditional energy sources such as petroleum and coal has grown rapidly. As shown in Figure 1, the data map of the US Energy Information Administration (EIA) shows that fossil fuels (66%) dominate the U.S. energy consumption, while the use of photovoltaic power generation is only 1%. However, burning fossil fuels is not a sustainable energy production method because these energy sources are limited. In addition, the process of harvesting energy releases a large amount of greenhouse gases and other pollutants. [1]



Source: U.S. Energy Information Administration

Fig.1.1 Pie chart of 2014 US net generation by energy source

As early as 1839, French scientist Becquerel discovered that light produced a potential difference between different parts of a semiconductor material. This phenomenon was later called "photovoltaic effect" and was called "photovoltaic effect." In 1954, American scientists Chao Yang and Russell Ohl produced the first practical monocrystalline silicon solar cell at Bell Labs in the United States, creating a practical photovoltaic power generation technology. The technology that converts sunlight energy into electricity.

Since the 1970s, with the development of modern industry, the global energy crisis and atmospheric pollution have become increasingly prominent. The decreasing use of traditional fuels and energy has caused more and more serious damage to the environment. At the same time, about 2 billion people in the world cannot enter the normal energy supply. At this time, the world has turned its attention to renewable energy. It is hoped that renewable energy can change human energy structure and maintain long-term sustainable development. Among them, solar energy has become the focus of attention with its unique advantages. Rich solar radiation energy is an important energy source. It is inexhaustible, pollution-free and cheap. Humans can use energy freely. Solar energy can reach 80 million kilowatts of ground per second. If 0.1% of the solar energy on the surface of the Earth is converted into electricity, the conversion rate will reach 5%, and 5.6×10^{12} kWh of electricity will be generated each year, which is equivalent to 40 times of the world's energy consumption. Thanks to these unique solar advantages, after the 1980s, the types of solar cells have been increasing, the scope of application has become wider and wider, and the market scale is gradually expanding.

After the 1990s, photovoltaic power generation developed rapidly. By 2006, more than 10 MW photovoltaic power generation systems and 6 MW photovoltaic grid-connected power plants have been built in the world. The United States was the first country to develop a photovoltaic power generation development plan. 1997 also put forward the "million roof" plan. Japan started a new sunshine plan in 1992. As of the end of 2003, Japan's PV module production accounted for 50% of the world total. Four

of the top 10 manufacturers in the world are in Japan. The German Renewable Energy Law provides tariffs for photovoltaic power generation, which greatly promotes the development of the photovoltaic market and industry, making Germany the fastest growing country in the world after Japan. Countries such as Switzerland, France, Italy, Spain, and Finland have also formulated photovoltaic development plans, vigorously developed the technology industry, and accelerated the pace of industrialization. [2]

The average annual growth rate of PV modules from 1990 to 2005 is about 15%. In the late 1990s, the pace of development was faster, and photovoltaic modules reached 200 MW in 1999. The efficiency of commercial batteries increased from 10% to 13%, from 13% to 15%, and the scale of production expanded from 1 to 5 MW/year, reaching 5 to 25 MW/year, and towards 50 MW or even 100 MW. The direction of expansion. The cost of producing PV modules has fallen below \$3/watt. [3]

Chapter 2 Introduction

Photovoltaic power generation is a technology that uses the photovoltaic effect of a semiconductor interface to directly convert light energy into electrical energy. The key component of this technology is solar cells. The solar cells can be connected in series to form a large-area solar cell module and then form a photovoltaic power generation device together with components such as an upper power controller. [4]

Solar photovoltaic modules convert direct sunlight into direct current. The PV string is connected in parallel to the DC distribution cabinet through the DC combining box, and then the DC string is connected to the DC input of the inverter, and the DC power is converted into AC power. The AC output terminal of the inverter is connected to the AC power distribution cabinet, and the AC power distribution cabinet directly enters the user side.

2.1 System classification

Photovoltaic power generation systems are divided into independent photovoltaic systems and grid-connected photovoltaic systems.

Independent photovoltaic power plants include various types of photovoltaic power generation systems, such as rural power supply systems for remote photovoltaic power stations, home solar power systems, communications signal power supplies, cathodic protection, and solar street lights. [5]

The grid-connected photovoltaic power generation system connects the power grid and power transmission to the grid photovoltaic power generation system. Can be

2.2.1 PV Array

Solar cells are devices that convert light energy directly into electrical energy through photovoltaic or photochemical effects. As long as it is illuminated by light that satisfies certain lighting conditions, it can instantaneously output voltage and generate current in the presence of a loop. Physically referred to as photovoltaic (PV).

The principle of solar cells is the photoelectric effect + p-n junction. When the sun shines on the p-n junction of the semiconductor, new hole electron pairs are formed. Under the action of the built-in electric field of the p-n junction, photogenerated holes flow to the p region, and photogenerated electrons flow to the n region. After the circuit is turned on, electric energy is generated. Specifically, it is non-conductive. If different impurities are buried in a semiconductor that is not conductive, then P-type (boron and other impurities) and N-type (phosphorous, etc.) semiconductors. The potential difference between the hole of the p-type semiconductor (a p-type semiconductor has one negatively charged electron, which can be regarded as one more positive charge) and one free electron of the n-type semiconductor generates electric energy. Therefore, when sunlight shines, light energy excites electrons in the silicon atom (photoelectric effect), and convection of electrons and holes are generated. These electrons and holes are affected by the built-in potential, and are respectively accumulated in the N type. And P-half two-section, at this time if the external connection with the electrode can form a loop, which is the current mainstream solar cell principle.^[8]

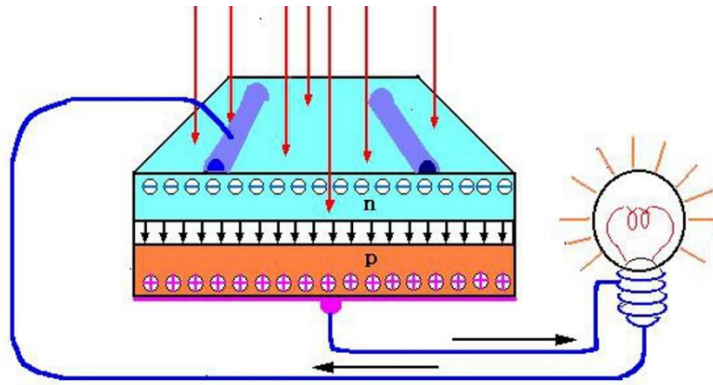


Fig.2.2 The principle of solar cells

Since the electricity generated by the solar battery is a direct current, if it is necessary to supply electric energy to a household appliance or various electric appliances, a direct/ac converter must be installed to convert the direct current into an alternating current to provide electric energy. Household appliances or industrial electricity.

2.2.2 Controlling Device

It can automatically prevent over-charging batteries and over-discharge devices. Since the battery charge and discharge times and discharge depth are important factors in determining the battery life, it is possible to control the battery pack overcharge or overdischarge controller is an indispensable charge and discharge equipment.

MPPT

As shown in Figure 2.3, an independent photovoltaic power generation system with MPPT control function is proposed. In order to achieve MPPT, the traditional algorithm needs to simultaneously detect the output voltage and output current of the photovoltaic cell. The basic principle of the incremental conductance method is briefly described below. [9]

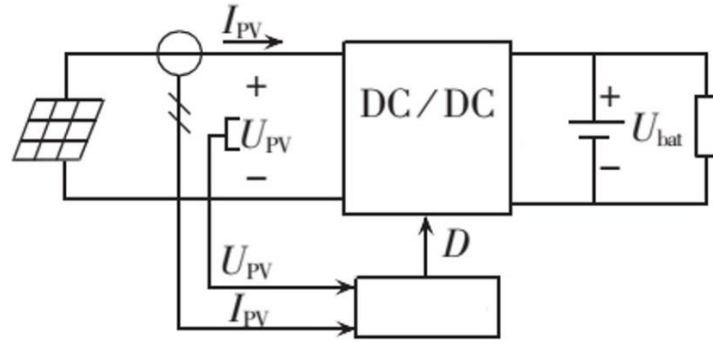


Fig.2.3 Stand-alone photovoltaic system with MPPT

Incremental conductance method is one of the common methods of photovoltaic array MPPT. From the $P - U$ curve of the PV array, its slope at the maximum power point is zero and $P = UI$, so at the maximum power point there is:

$$\frac{dP}{dU} = \frac{d(IU)}{dU} = I + U \frac{dI}{dU} = 0$$

which is

$$\frac{dI}{dU} = -\frac{I}{U}$$

That is to achieve the maximum power point conditions. If:

$$\frac{dI}{dU} < -\frac{I}{U}$$

The operating point of the PV module is located on the right side of the maximum power point. At this time, the output voltage should be reduced. If:

$$\frac{dI}{dU} > -\frac{I}{U}$$

The operating point of the PV module is on the left side of the maximum power point. At this time, the output voltage should be increased.

When the algorithm has high control accuracy, rapid response and changes in solar irradiance, the output voltage of the PV array can stably track its changes, and the steady state oscillation is smaller than the disturbance observation method. Photovoltaic cell

arrays and loads are connected via DC / DC circuits. The maximum power tracking device continuously detects the current and voltage changes of the photovoltaic array and adjusts the duty cycle of the PWM drive signal of the DC/DC converter according to the change.

2.2.3 Boost Converter

A DC-DC converter is an electrical device that converts a DC input voltage into a high DC output voltage. It uses a control circuit to generate a switching signal modulated by an error signal to control the opening and closing of the power switch, and then utilizes energy storage and energy release of the inductor, capacitor and diode to achieve energy conversion. The PWM control circuit can control the turn-on and turn-off of the IGBT. The DC voltage output from the photovoltaic array is boosted by the DC/DC converter and the output DC voltage is used as the input voltage of the inverter. The DC/DC converter is mainly composed of switching elements such as reactors, diodes, and IGBTs, since the MPPT control needs to maximize the power obtained from the solar cells, so the input voltage is controlled optimally by the PWM control. [10]

Figure 2.4 shows the topology of the main circuit of the Boost converter. It is mainly composed of a power switch M, an inductor L, a freewheeling diode D1, a load capacitor C, and a load R. The resistor R_L is the DC resistance of the inductor and R_C is the equivalent resistance of the load capacitor.

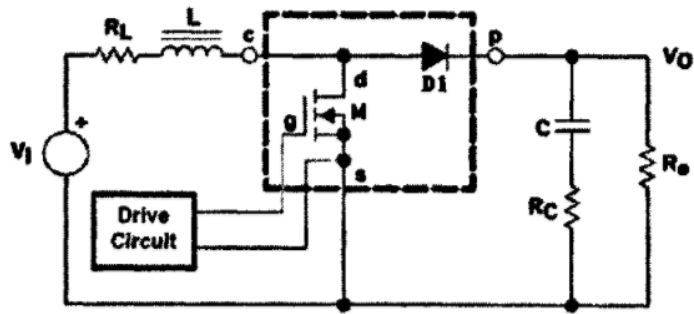


Fig.2.4 The main circuit of boost converter

Its working process is divided into two phases. When the switch is on, the main current loop includes inductors, switches, and an input voltage source. The on-time of the switch is T_{on} , as shown in Figure 2.5(a). When the switch is turned on, the on-resistance R_{DSON} of the switch M is very small. The right end of the inductor is equivalent to the ground, the left end is connected to the power supply voltage, the current flowing through the inductor rises linearly with a fixed slope, energy is stored in the inductor in the form of magnetic energy; the freewheeling diode D1 is reverse biased; in the off state Next, the capacitor C discharges through the load R_O to provide energy to the load. When the switch is open, the main current loop includes the inductor, diode, capacitor, load, and input voltage source. The off-time of the switch is T_{OFF} , as shown in Figure 2.5(b). During the T_{OFF} phase, the current in the inductor cannot be abrupt, so the diode opens immediately in the positive direction. At this point, the voltage at which the inductor is connected to the switch is clamped by the output voltage. This voltage is called the flyback voltage and the amplitude is the output voltage minus the forward voltage drop of the diode. The inductance is released to the load through the freewheeling diode D1 magnetic energy and charges the load capacitance.

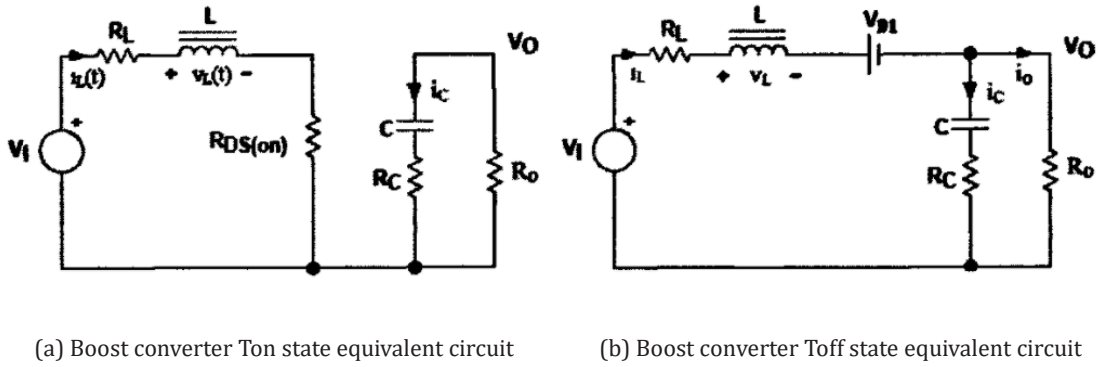


Fig.2.5 Boost converter working condition analysis

Inductive switching DC-DC converters use magnetic field energy storage to achieve maximum power conversion efficiency, whether step-up, step-down, or both. Although it requires a larger board area than a linear or charge pump device, it is ideal for applications that require more current. Due to the high conversion efficiency, the heat generation is very small, which also simplifies the heat treatment. In particular, it generally does not require the addition of large space-consuming, cost-effective heat sinks when compared to LDO devices. Its high efficiency of up to 97% also improves battery life. The DC-DC converter also appears as a DC-DC controller, which guarantees design flexibility. Considering the output capability and efficiency of FET-based inductive switching mode DC-DC converters, only external inductors and indispensable output capacitors are required for use, which greatly increases the space utilization of the entire solution.

With the development of semiconductor technology and the integration and continuous improvement of switching frequency, the sizes of inductors and capacitors in DC-DC converters and peripheral devices have been continuously reduced, and the cost has been gradually reduced. At present, DC-DC converters have gradually become

an attractive power supply solution. With the continuous development of electronic technology and continuous development of new products, the integration of DC-DC conversion power chips, energy conversion efficiency, and output noise reduction will continue to be the goals pursued by people.

2.2.4 DC-AC Inverter

It is a DC conversion device for AC power. Since solar cells and batteries are DC power supplies and the load is AC load, inverters are essential. The inverter operation mode can be divided into independent inverters and grid-connected inverters.

Three-phase voltage type inverter circuit

Three single-phase inverter circuits can be used to combine three-phase inverter circuits. However, in the three-phase inverter circuit, the most widely used three-phase bridge inverter circuit is used. The use of IGBTs as three-phase voltage bridge inverter switching devices, as shown in Figure 2.6, can be considered as a three-half-bridge inverter circuit. [11]

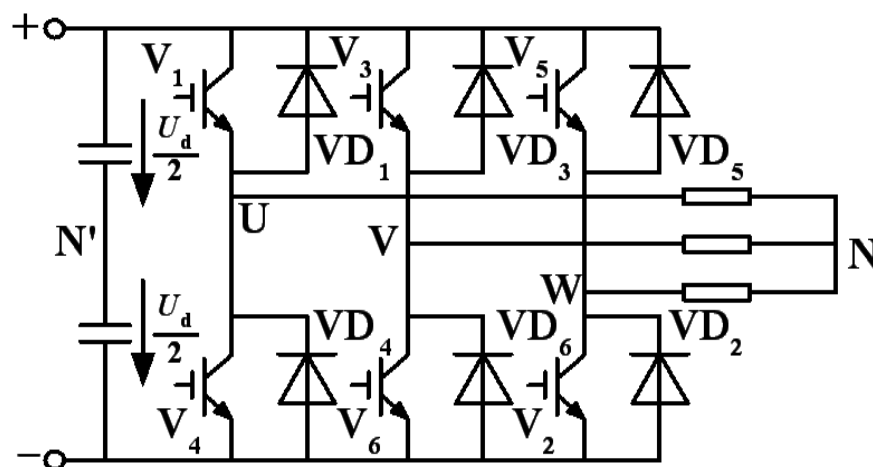


Fig.2.6 Three-phase voltage bridge inverter circuit

The DC side of the circuit is usually only a capacitor on it, but for the convenience of analysis, draw two capacitors in series and marked the imaginary mid-point N. And the single-phase half-bridge, full-bridge inverter circuit the same three-phase voltage bridge inverter circuit is also the basic 180 degree conductive mode, that each leg of the conductive angle of 180, the same phase (that is, the same half-bridge) The upper and lower arms alternately conduct electricity, and the phases begin to differ in conductivity by 120 degrees. In this way, at any moment, there will be three bridge arm conduction at the same time. It may be two arms below the one arm, or one arm below the two arms at the same time. Because each commutation is carried out on the same phase between two bridge arms, it is also called longitudinal commutation.

The following analysis of three-phase voltage bridge inverter operating waveform. For the U phase output, when the arm 1 is on, $U_{UN'}=U_d/2$, when the arm 4 is on, $U_{UN'}=-U_d/2$. Therefore, the waveform of $U_{UN'}$ is a square wave of amplitude $U_d/2$. The case of V and W phases is similar to that of U phase. The shape of $U_{VN'}$ and $U_{WN'}$ is the same as that of $U_{UN'}$, except that the phases are in turn 120° . Load line voltage can be obtained by the following formula:

$$\begin{cases} U_{UN} = U_{UN'} - U_{NN'} \\ U_{VN} = U_{VN'} - U_{NN'} \\ U_{WN} = U_{WN'} - U_{NN'} \end{cases}$$

Assuming that the voltage between the load midpoint N and the imaginary midpoint N' of the DC power supply is $U_{NN'}$, the phase voltages of the phases of the load are respectively:

$$\begin{cases} U_{UN} = U_{UN'} - U_{NN'} \\ U_{VN} = U_{VN'} - U_{NN'} \\ U_{WN} = U_{WN'} - U_{NN'} \end{cases}$$

Three-phase voltage bridge inverter operating waveform shown in Figure 2.7.

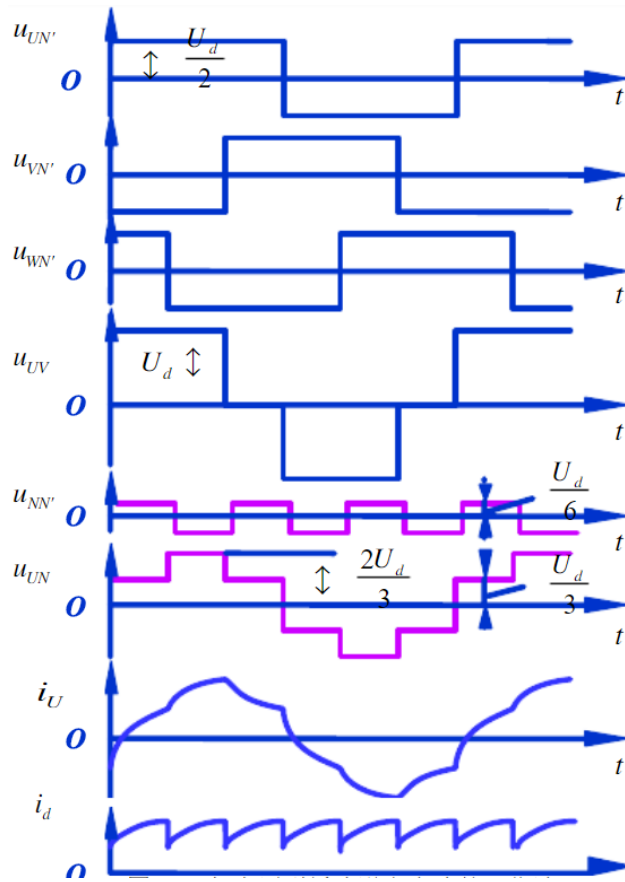


Fig.2.7 Three-phase voltage bridge inverter operating waveform

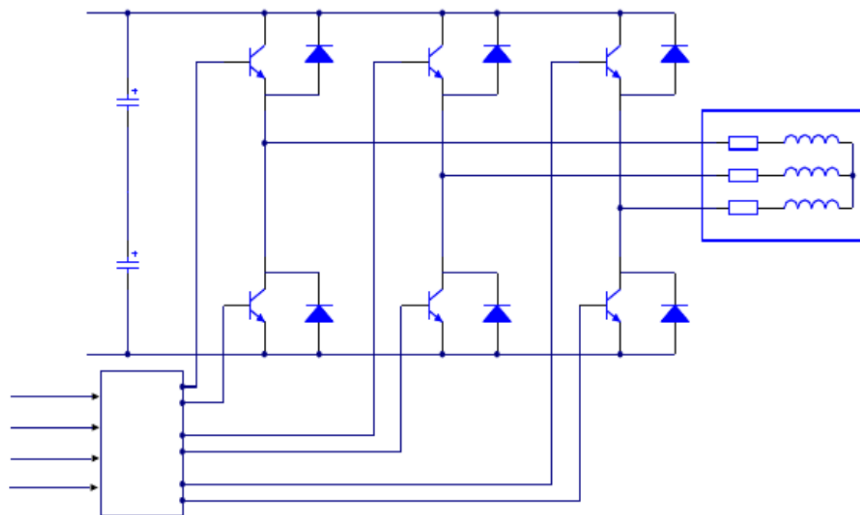


Figure 2.8 The main circuit design of SPWM inverter

Figure 2.8 is the main circuit design of SPWM inverter. VI-V6 in the picture is the six power switching devices of the inverter, each anti-parallel diode is connected in parallel, and the whole inverter is powered by the constant DC voltage U . A set of three-phase symmetrical sinusoidal reference voltage signals are referenced to the fundamental frequency and should be adjustable over the desired output frequency range. The magnitude of the reference signal can also vary within a certain range, determining the size of the output voltage. Triangular carrier signal U_c is common, respectively, compared with each phase reference voltage, given a "positive" or "zero" of the saturated output to generate SPWM pulse sequence wave. U_{da} , U_{db} , U_{dc} as the inverter power switching device drive control signal.

Three-phase bridge voltage inverter circuit summary:[12]

- (1) The line voltage is a rectangular wave, the phase voltage is a staircase wave.
- (2) Each phase output voltage difference in phase 120°, the current waveform according to the different load conditions.
- (3) Three-phase bridge voltage inverter circuit used in high-power applications.
- (4) The output voltage waveforms are rectangular wave, regardless of the load, and the current waveform and phase are different due to the different load impedance angle.
(Rectangular wave, or approximately a sine wave)
- (5) When the load is inductive, it is necessary to provide reactive power. The DC side capacitor serves as a buffer for the reactive energy. To provide a channel for the AC side to feed back the DC side feedback energy, each arm must be connected in parallel with a feedback diode.

2.2.5 Grid

The entire substation consists of transmission lines and distribution lines in voltage substations and power systems, which are called grids. It includes substations, transmission and distribution units. The task of the grid is to transmit and distribute electrical energy and change the voltage. [13]

Chapter 3 MODELING

3.1 MATLAB Simulink

MATLAB is a set of large-scale high-performance numerical calculation and visualization software developed by MathWorks in the United States. It is based on matrix operations and integrates calculation, visualization, and program design in an interactive work environment. In this environment, it can be achieved. Engineering calculation, algorithm research, modeling and simulation, and application development have been widely used in scientific computing, engineering design, and system simulation. In MATLAB, there are two main parts, mathematical calculations and engineering simulations. Among them, the software support provided by MATLAB involves various engineering fields and is continuously improved. MATLAB has flexible, intuitive and powerful graphics features, making it a multi-disciplinary, multi-platform powerful large-scale software. The SIMULINK toolbox provided by MATLAB is a software package that models, simulates, and analyzes dynamic systems in the MATLAB environment. It provides an interface modeled with a block diagram that is more intuitive than traditional simulation modeling. flexible. Simulink's role is to create a system based on street-level interconnection. Each program block consists of three elements: input vectors, output vectors, and vectors that represent state variables. Before the calculation, initial values need to be initialized and assigned, and the blocks are sorted according to the order in which they need to be updated. The ODE calculation program is then used to numerically integrate the system. MATLAB

contains a large number of ODE calculation programs, with a fixed step size and variable step size, to facilitate the solution of complex systems. The application of MATLAB in power system modeling and simulation is mainly performed by the power system simulation module SIMPOWER.

MATLAB is a powerful platform for integrated computing, visualization and programming. Power system simulation models and models, the power system simulates the actual operation of the power system. Because the power system is a complex system and its operation mode is also very complicated, it is not intuitive to use the traditional method for simulation calculation. The emergence of MATLAB has brought new methods and methods for power system simulation. The SIMPOWER system module of MATLAB is used to simulate the application of power system. It shows that the application of power system simulation in power system simulation is helpful for people to analyze the actual operation of power system through computer means. The related voltage stability conclusion proves the correctness of the simulation and its feasibility in the application of analysis.

3.2 PV Array

Solar photovoltaic power generation system uses solar photovoltaic materials semiconductor materials to directly convert solar photovoltaic energy into new generation systems. Due to the high cost, computer simulation technology has become an effective way to study such systems. In fact, the solar radiation is unstable. There are usually three ways to establish the mathematical models of photovoltaic arrays: one is to directly evaluate the PV array as a DC voltage source. This method is the simplest,

but it can not track the changes of solar radiation intensity, environmental temperature and output of PV array, nor can it reflect the characteristics of PV array. The other method is based on the volt ampere characteristic method of photovoltaic array, and modifies the open circuit voltage, short circuit current and the fitting curve coefficient, so that the relationship between the model characteristics and the actual photovoltaic array is similar to the different light and temperature characteristics, but it is more difficult to set the temperature, and the light is more difficult to set up the base of the mathematical model of the photovoltaic array. A physical model is established to describe the internal characteristics of the PV array to simulate the changes of the external environment.

Figure 3.1 shows the equivalent photovoltaic cell model, which consists of the ideal current source I_{sc} , the antiparallel diode V_D , the series resistor R_s and the shunt resistor R_{sh} . The value of I_{sc} is equal to the short-circuit current of the battery, and its size reflects the solar irradiance of the environment in which the photovoltaic cell is located. The stronger the sunshine is, the larger the I_{sc} is and vice versa.[14]

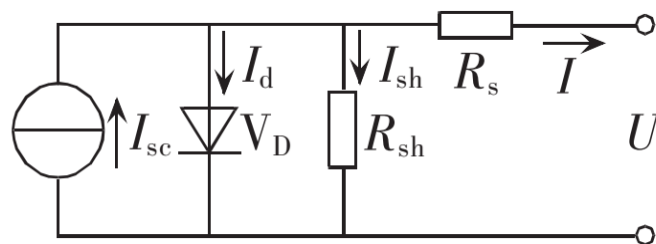


Fig.3.1 Equivalent circuit of photovoltaic cell

When the light intensity is constant, the photocurrent I_{ph} does not change with the working state of the photovoltaic cell, so it can be regarded as a constant current source in the equivalent circuit. After both ends of the photovoltaic cell are connected to the

load R, the photocurrent flows through the load, so that the terminal voltage V is established at both ends of the load. The load terminal voltage reacts on the PV cell's P - N junction, producing a current I_d opposite to the photocurrent direction. In addition, due to the electrodes on the front and back surfaces of the solar photovoltaic panels and the resistivity of the materials themselves, the series resistance R_s is introduced when the operating current flows through the board and inevitably causes a series loss in the panel. The greater the series resistance, the greater the line loss, the lower the output efficiency of photovoltaic cells. In the actual solar photovoltaic cells, the general series resistance is relatively small, mostly in a few micro-European to a few European between. In addition, due to the manufacturing process, the edge of the photovoltaic cell and the metal electrode may be produced in the production of small cracks, scratches, which will form a leakage current that led to the original photocurrent will flow through the load short-circuit, so the introduction of a parallel resistance R_{sh} to be equivalent. Relative and series resistance, parallel resistance is relatively large, generally more than $1k\Omega$.

The following equation can be drawn by the solar photovoltaic cell equivalent circuit:

$$I = I_{ph} - I_d - I_{sh}$$

Where I is the current flowing through the load, that is, the output current of the photovoltaic module; I_{ph} is the photo-generated current proportional to the sunshine intensity; I_d is the current flowing through the diode; I_{sh} is the leakage current of the

solar photovoltaic cell. According to the theory of electronics, the physical properties of the material determine the ideal diode solar cell I - V characteristics:

$$I_d = I_0 \left\{ \exp \left[\frac{q(V + IR_s)}{AKT} \right] - 1 \right\}$$

Where V is the voltage across the load, that is, the output voltage of the PV module; I₀ is the diode saturation current (in general, it is on the order of 10⁻⁴A); q is the charge capacity (1.6 x 10⁻¹⁹ C); A is the diode performance index, that is, P-N junction ideal factor; K is the Boltzmann constant (1.38 × 10⁻²³ J / K); T is the absolute temperature (= t + 273 K); R_s is the photovoltaic cell series resistance; R_{sh} is Pool parallel resistance.

In addition,

$$I_{sh} = \frac{V + IR_s}{R_{sh}}$$

Therefore, the general formula (2) ~ formula (4), we can get:

$$I = I_{sc} - I_0 \left\{ \exp \left[\frac{q(V + IR_s)}{AKT} \right] - 1 \right\} - \frac{V + IR_s}{R_{sh}}$$

Where T is the absolute internal battery temperature; V is the photovoltaic cell output voltage; I₀ is the diode saturation current; R_{sh} is the internal shunt resistance; R_s is the internal series resistance; q is the electron charge, q = 1.602 × 10⁻¹⁹ C; A is Diode factor, usually 1 ~ 3; k is the Boltzmann constant, k = 1.380 58 × 10⁻²³ J; n is the number of cells in series.

According to Eq. (1), a simulation model of PV cell is established as shown in Fig.3.2

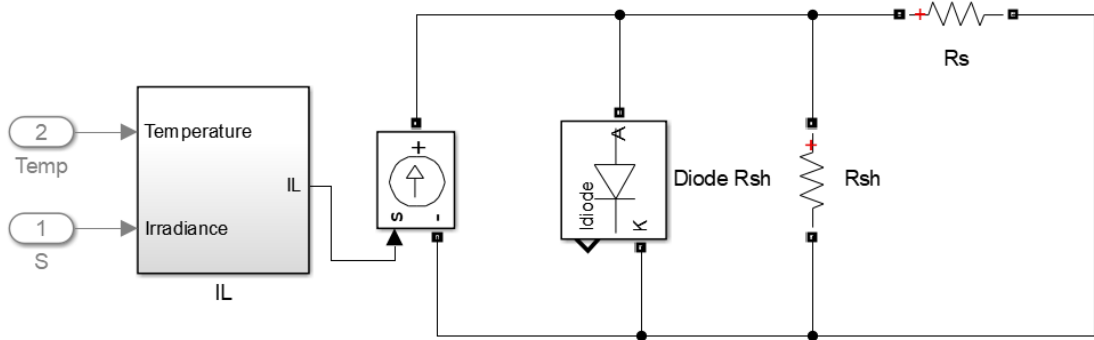


Fig.3.2 Simulation model of PV cell

3.2.1 Light Generated Current

When the light intensity is constant, the light-generated current IL does not change with the working status of PV cells, so it can be simulated by a constant current source.

We will use the following formula Eq to simulate light generated current:[15]

$$IL = \frac{S}{S_{ref}} * (IL_{ref} + \alpha_{isc} * (T_{cell_K} - T_{ref_K}))$$

In the formula, S is the radiation intensity (W/m^2), $S_{ref}=1000W/m^2$ is the reference value of the radiation intensity in the standard state, IL_{ref} is the photocurrent of the component in the standard state, α_{isc} is the temperature parameter value, T_{cell_K} is the battery Current temperature (K), T_{ref_K} is the temperature in the standard state ($25C^\circ$).

The figure 3.3 below shows the matlab simulation model, using math module to calculate the photocurrent formula.

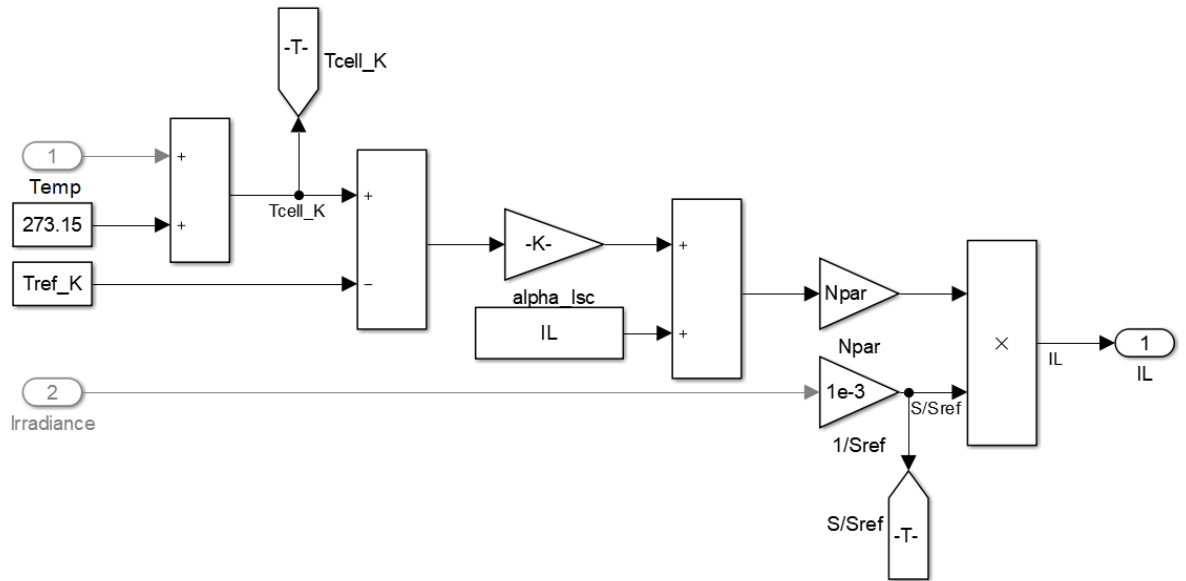


Fig.3.3 Simulation model of light generated current

And we can see the plot below, the two figures on the left are the temperature and irradiance, and the one on the right is the resulting photocurrents.

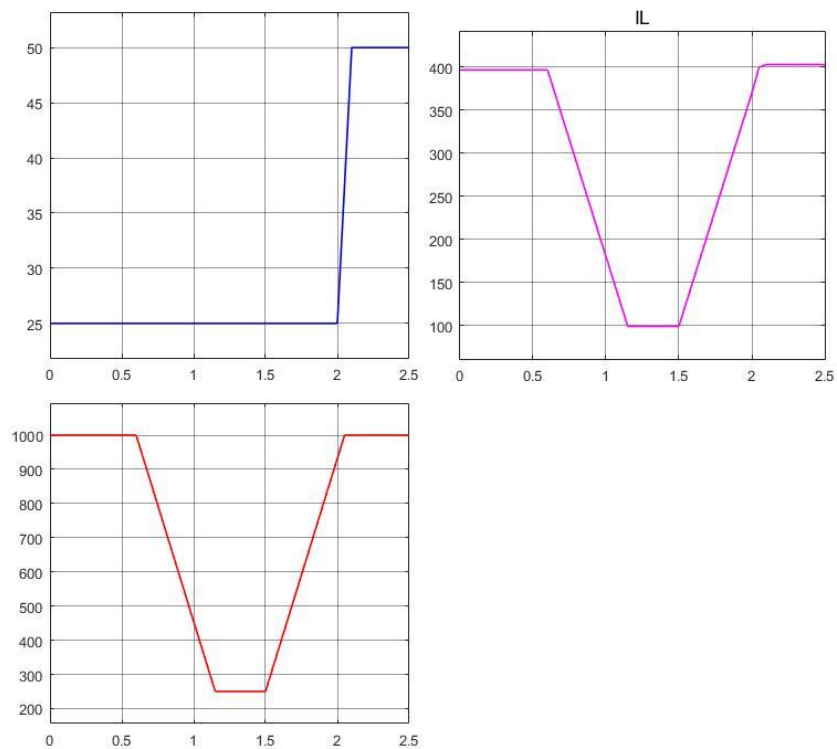


Fig.3.4 The waveform of temperature and solar irradiance and the resulting photocurrent

3.2.2 Controlled Current Source

The formula derived from the previous:[16]

$$I = I_{sc} - I_0 \left\{ \exp \left[\frac{q(V + IR_s)}{AKT} \right] - 1 \right\} - \frac{V + IR_s}{R_{sh}}$$

As you can see, we want to get I, so in MATLAB we can set the Diode and R_{sh} parts together as a controlled current source to generate $I_d + I_{sh}$. Here we can use a new way to calculate the I_d :

$$I_d = I_0 * \left[\exp\left(\frac{V_d}{V_T}\right) - 1 \right]$$

Where V_d is the voltage of diode which we can measure, and V_T is the temperature voltage:

$$V_T = k * T_{cell_K} / q * n * N_{cell} * N_{ser}$$

Similarly, use MATLAB to get the current $I_d + I_{sh}$ as shown in the figure 3.5 below:

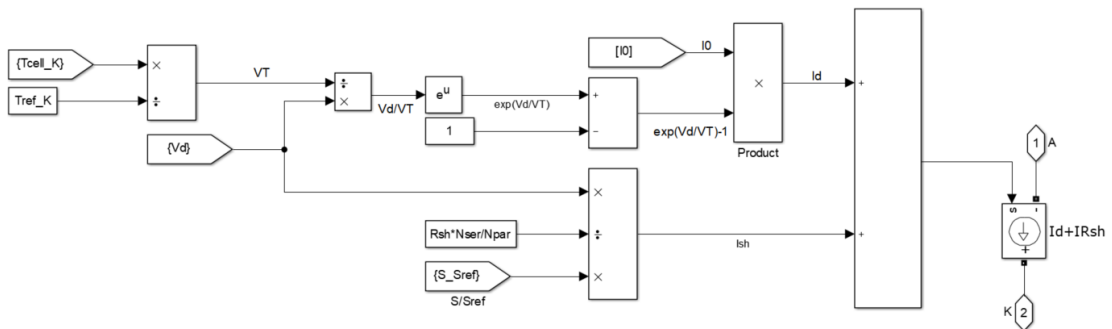


Fig.3.5 Simulation model of controlled current source

3.3 MPPT Controller & Boost Converter

Therefore, after completing the simulation of the PV circuit, we want to use the maximum power point tracking method to control the output voltage, and use the boost inverter to increase the voltage.

The MPPT controller uses incremental conductance and integral regulator technology to optimize switching duty cycle. The duty ratio of the converter is obtained from the MPPT controller. The incremental conductance method is an incremental algorithm. By associating the PV module's conductance (I / V) with its enhanced conductance (dI / dV), the control variables can be reduced and increased properly. The maximum power point is obtained when photovoltaic power is generated. [17]

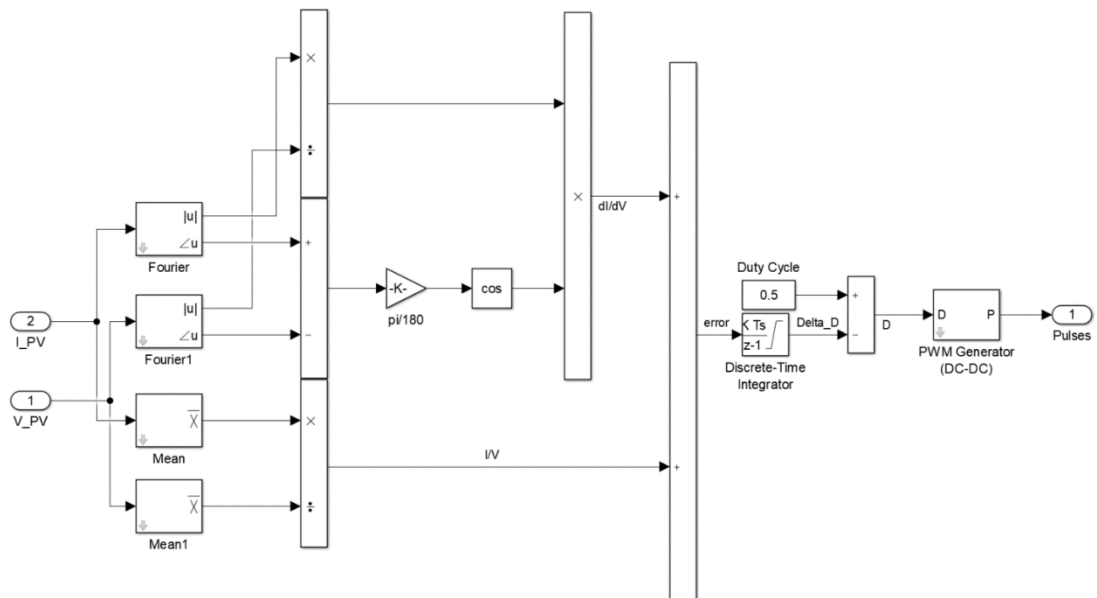


Fig.3.6 Simulation model of using INC algorithm to build PWM

From the above figure 3.6, we can see that I use the incremental conductance algorithm and use the integrator to minimize $dI / dV + I / V$, so we get the duty ratio. Then I use this duty cycle to set up PWM, which can be used to generate trigger pulses

to drive switches. As shown below, the output voltage level can be adjusted by changing the duty cycle of the PWM, so that the output voltage can track the maximum power point voltage. If the working voltage is on the left of the maximum power point voltage, the duty ratio is increased to make the working voltage close to the maximum power point voltage; otherwise, the duty ratio is reduced.

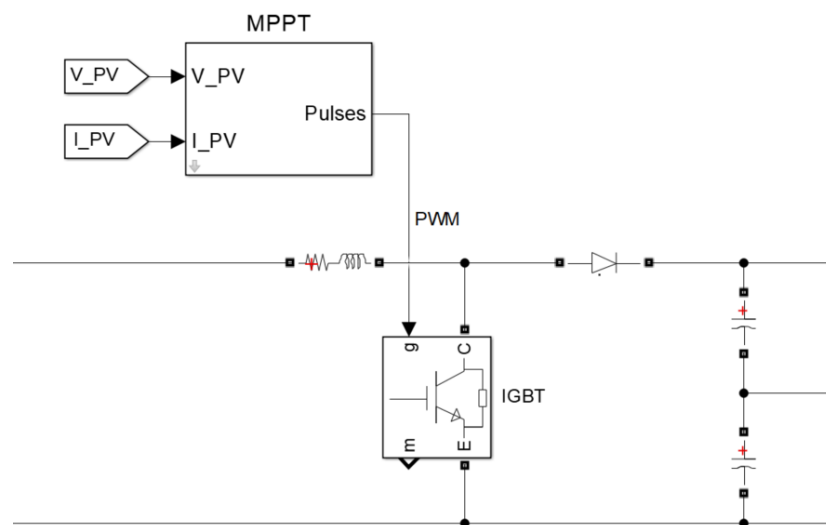


Fig.3.7 Simulation model of general boost converter with MPPT

The process of rising pressure is a process of induction energy transfer. When charging, the inductor absorbs energy and releases energy when the inductor discharges. If the capacitance is large enough, a constant current can be maintained during discharge. If the switching process is repeated, the voltage higher than the input voltage can be obtained at both ends of the capacitor.

3.4 VSC

The inverter output current that is injected into the utility network must be synchronized with the grid voltage. The objective the synchronization algorithm is to extract the phase angle of the grid voltage. The feedback variables can be converted into a suitable reference frame using the extracted grid angle. Hence, the detection of the grid angle plays an essential role in the control of the grid-connected inverter. The synchronization algorithms should respond quickly to changes in the utility grid. Moreover, they should have the ability to reject noise and the higher order harmonics. Many synchronization algorithms have been proposed to extract the phase angle of the grid voltage such as zero crossing detection, and phase-locked loop (PLL).[18]

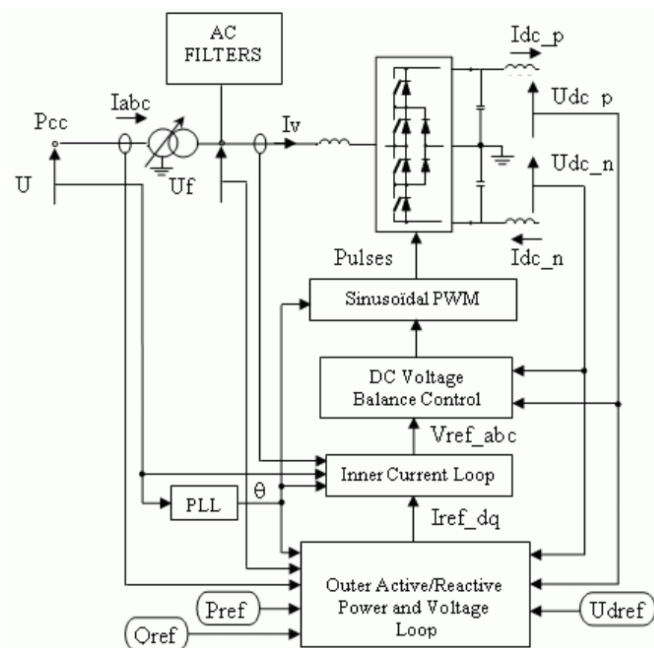


Fig.3.8 The general design model of VSC

Source: mathswork

The voltage outer loop and the current inner loop control the constant voltage and the constant current, which is a control method in the PWM rectification, and belongs

to the feedback description term of the hysteresis current control such as the direct current control. The purpose of direct current control is that the inner loop uses current to closely track the input voltage waveform, and tracking is hysteresis. Current hysteresis achieves AC synchronization and achieves unity power factor relative to prediction. The purpose of the voltage outer loop is to compare the output voltage and the effective value of the input voltage to determine the flow of control power of the PWM, so as to achieve bidirectional double-fed control of the voltage.

3.4.1 PLL

PLL synchronization method is a closed-loop system, which is widely used in the grid-connected systems. The basic task of the phase-locked loop is to quickly and accurately detect the grid signal and track the frequency and phase of the grid signal. Typically, a PLL system consists of a Phase Detector(PD), a Loop Filter(LF) which is performed by a Proportional Integrator(PI) controller, and a Voltage Controlled Oscillator (VCO).^[19]

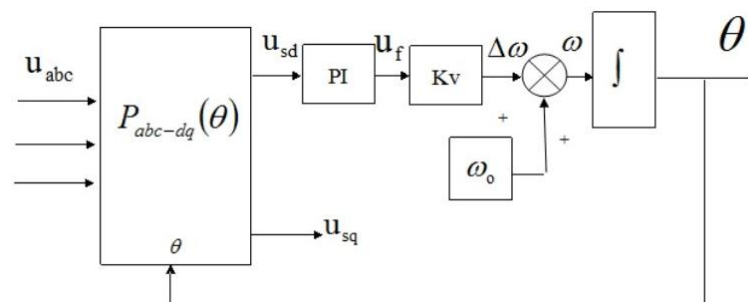


Fig.3.9 Phase-locked loop

The accuracy of the phase signal output from the phase-locked loop is directly related to the control performance of the current controller until it is determined whether

it can work normally, and because the harmonics and other factors are generated due to the action of the inverter switching device, the required phase-locked loop is required. Not only must have the characteristics of fast response, no steady-state error, but also can suppress harmonics and have a wider frequency band.

The characteristics of the phase-locked loop structure are: (1) When the phase is locked, the phase error u_{sd} is constant, that is, there is no lower harmonic into the low-pass filter, so the frequency of the phase-locked loop can be satisfied as much as possible in the parameter design. Locking range and response speed; (2) The low-pass filter in the figure uses a PI regulator structure to not only play a low-pass filter but also ensure phase tracking without steady-state errors.

Phase Detector

The phase detector of the PLL is implemented by rotating the d-q coordinates. The three-phase grid voltage vector u transforms the stationary three-phase coordinate system into the two-phase orthogonal stationary vectors $U\alpha$, $U\beta$ by the Clark transformation method. Assume that the three-phase voltages Ua , Ub , and Uc are in ideal states, so that they can be obtained after normalization:

$$U_{abc} = \begin{bmatrix} Ua \\ Ub \\ Uc \end{bmatrix} = \begin{bmatrix} \cos\theta_1 \\ \cos\left(\theta_1 - \frac{2}{3}\pi\right) \\ \cos\left(\theta_1 + \frac{2}{3}\pi\right) \end{bmatrix}$$

Where θ_1 is the input phase angle of the grid

By transforming the stationary coordinate system, the stationary three-dimensional coordinate system is converted into a stationary two-dimensional coordinate system: the three-phase voltage vector is projected onto the stationary α and β coordinate systems.

$$T_{\alpha\beta} = \frac{2}{3} \begin{bmatrix} 1 & -\frac{1}{2} & -\frac{1}{2} \\ 0 & \frac{\sqrt{3}}{2} & -\frac{\sqrt{3}}{2} \end{bmatrix}$$

Where $T_{\alpha\beta}$ is the transform matrix of the Clark transform.

Then, through the Park transformation, the two-dimensional stationary two-dimensional coordinates are converted into two-phase synchronous rotating two-dimensional coordinates, phase information is obtained, and the phase detection function is completed.

$$T_{dq} = \begin{bmatrix} \cos \theta & \sin \theta \\ -\sin \theta & \cos \theta \end{bmatrix}$$

$$U_{dq} = T_{dq} U_{\alpha\beta} = \begin{bmatrix} \cos(\theta_1 - \theta) \\ \sin(\theta_1 - \theta) \end{bmatrix}$$

$$U_d = \sin(\theta_1 - \theta)$$

Where T_{dq} is a synchronous coordinate transformation matrix.

The resulting q-axis component approaches zero, and the phase-locked loop achieves phase lock by controlling the q-axis component $U_d = 0$. When the phase is locked, the output phase angle tracks the input phase angle.

When $U_d > 0$, the d-axis delay U_{abc} , should increase the frequency of the synchronization signal; when $U_d < 0$, the d-axis advances U_{abc} , should decrease the

synchronization signal frequency; when $U_d = 0$, the d-axis and U_{abc} are in phase. Therefore, the phase can be completed by controlling u so that $U_d = 0$ to achieve the same phase between the two.

3.4.2 Outer Active-Reactive Power and Voltage Loop

For different control methods, there are different outer loop controllers. Since the selected control strategy only includes three methods: fixed active power control, fixed reactive power control, and constant DC voltage control, only the outer loop controller structure of these three control modes is discussed below.

(1) The outer ring active power and reactive power can be controlled. Under the condition of three-phase grid voltage balancing, let the grid

The voltage vector U_s is in the direction of the d-axis with $U_{sa}=U_s$ and $U_{sq}=0$.

$$P = 3/2 U_s * i_{sa}$$

$$Q = -3/2 U_s * i_{sq}$$

Therefore, it is possible to control p and q separately by means of i_{sa} and i_{sq} , so as to realize independent adjustment of active power and reactive power.

In order to eliminate the steady-state error and introduce a PI regulator, the reactive power controller mechanism of the active power controller is shown in the figure below.

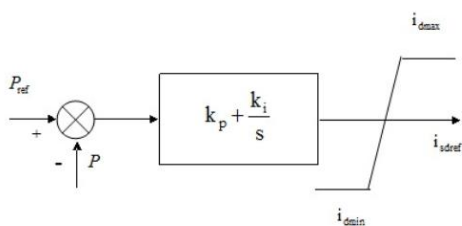


Fig.3.10(a) d-axis active power regulation

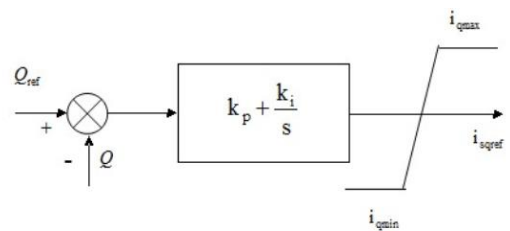


Fig.3.10(b) q-axis reactive power regulation

The deviation of the active power and active power command value in (a) above is converted into a reference amount of active current i_{sdref} after PI adjustment. Similarly, in Figure (b), the deviation between the reactive power and reactive power command values is adjusted by PI and converted into the reactive current reference quantity i_{sqref} .

(2) Outer loop DC voltage control. As mentioned above, the converter station adopting the constant DC voltage control mode can be used to balance the active power of the DC system and maintain the voltage stability of the DC side. Rectification of converters while neglecting R and converter losses

The active balance on both sides of the stream can be obtained by:

$$P=3/2U_s*i_{sd}=u_{dc}*i_{dc}$$

When the active power on both sides of the AC-DC converter is unbalanced, it will cause the DC voltage to fluctuate. At this time, the active power will charge (or discharge) the DC-side capacitor until the DC voltage stabilizes at the set value. Therefore, for a constant DC voltage controlled converter, it is equivalent to an active balancing node. The following figure shows the constant DC voltage controller. The deviation of the DC voltage and DC voltage commands is regulated by PI as the active current reference value i_{sdref} .

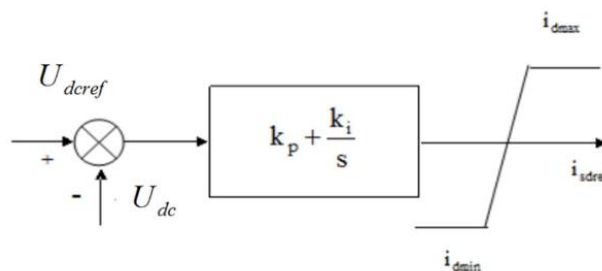


Fig.3.11 Constant DC voltage controlled converter

3.4.3 Inner Current Loop

According to the above formula, the dq axis current is controlled by the U_{rd} and the U_{rq} , and the two phase currents are coupled to each other. Therefore, a control method that can eliminate the current coupling between the dq axes needs to be found. From the above formula:

$$\begin{cases} U_d = -L \frac{di_{sd}}{dt} - Ri_{sa} + \omega Li_{sq} + U_{sa} \\ U_q = -L \frac{di_{sq}}{dt} - Ri_{sa} + \omega Li_{sa} + U_{sq} \end{cases}$$

In the equation, u_{sd} and u_{sq} are the d-axis and q-axis components of the PCC point voltage; u_d and u_q are the d-axis and q-axis components of the voltage fundamental wave on the AC side of VSC; i_{sd} , i_{sq} are the d-axis and q of the grid current, respectively. Axis components, R, L are the equivalent resistance and equivalent inductance of the connected transformer plus phase reactor. In addition to the effects of the controlled quantities u_d and u_q , the d-axis and q-axis currents are additionally affected by the current cross-coupling terms ωLi_{sd} , ωLi_{sq} and the grid voltages u_{sd} and u_{sq} . In order to eliminate the current coupling between the d-axis and the q-axis and the grid voltage disturbance, the equation can be rewritten in the form of the fundamental voltage of the desired output of the inverter on the AC side.

$$\begin{cases} U_d = U_{sd} - U'_d + \Delta U_q \\ U_q = U_{sq} - U'_q + \Delta U_d \end{cases}$$

where

$$\begin{cases} \Delta U_q = \omega Li_{sq} \\ \Delta U_d = \omega Li_{sd} \\ \begin{cases} U'_d = L \frac{di_{sd}}{dt} + Ri_{sa} \\ U'_q = L \frac{di_{sq}}{dt} + Ri_{sq} \end{cases} \end{cases}$$

In the formula, $u_{d'}$ and $u_{q'}$ are voltage components having a first derivative relationship with i_{sd} and i_{sq} , respectively. Obviously, this decoupling term can be implemented with the proportional-integral link shown in the following formula to compensate for the voltage drop across the equivalent reactor. The formula can be obtained by introducing the d-axis q-axis voltage coupling compensation terms u_d and u_q to decouple the nonlinear equations. At the same time, feedforward compensation is applied to the grid disturbance voltages u_{sd} and u_{sq} to realize the independence of the d-axis and q-axis currents. Decoupling control, but also improves the dynamic performance of the system. From the principle of control, the introduction of feedforward compensation in the formula actually uses open-loop control to compensate for the measurable disturbance signal.

$$\begin{cases} U'_d = K_{p1}(i^*_{sd} - i_{sd}) + K_{I1} \int (i^*_{sd} - i_{sd}) dt \\ U'_q = K_{p2}(i^*_{sq} - i_{sq}) + K_{I2} \int (i^*_{sq} - i_{sq}) dt \end{cases}$$

Therefore, the current decoupling controller shown in the figure 3.13 below can be obtained from the above formula. According to the voltage reference component and the grid voltage phase signal, the trigger pulse of each bridge arm can be obtained through pulse width modulation. The current reference value i_{sa}^* , i_{sq}^* in the figure from the outer ring

Controller output is obtained. Inner-loop current control adopts current feedback and grid voltage feed-forward to improve the current controller

Trace the corresponding characteristics, and at the same time through the PI regulator eliminates the current tracking steady-state error.

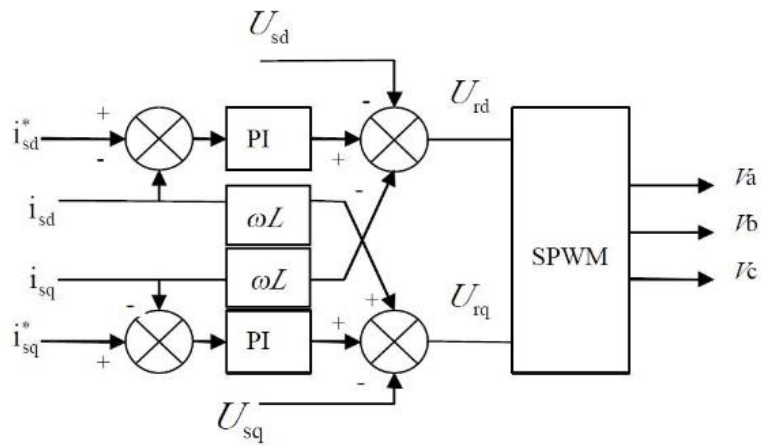


Fig.3.12 The inner current decoupling controller

3.4.4 Modeling

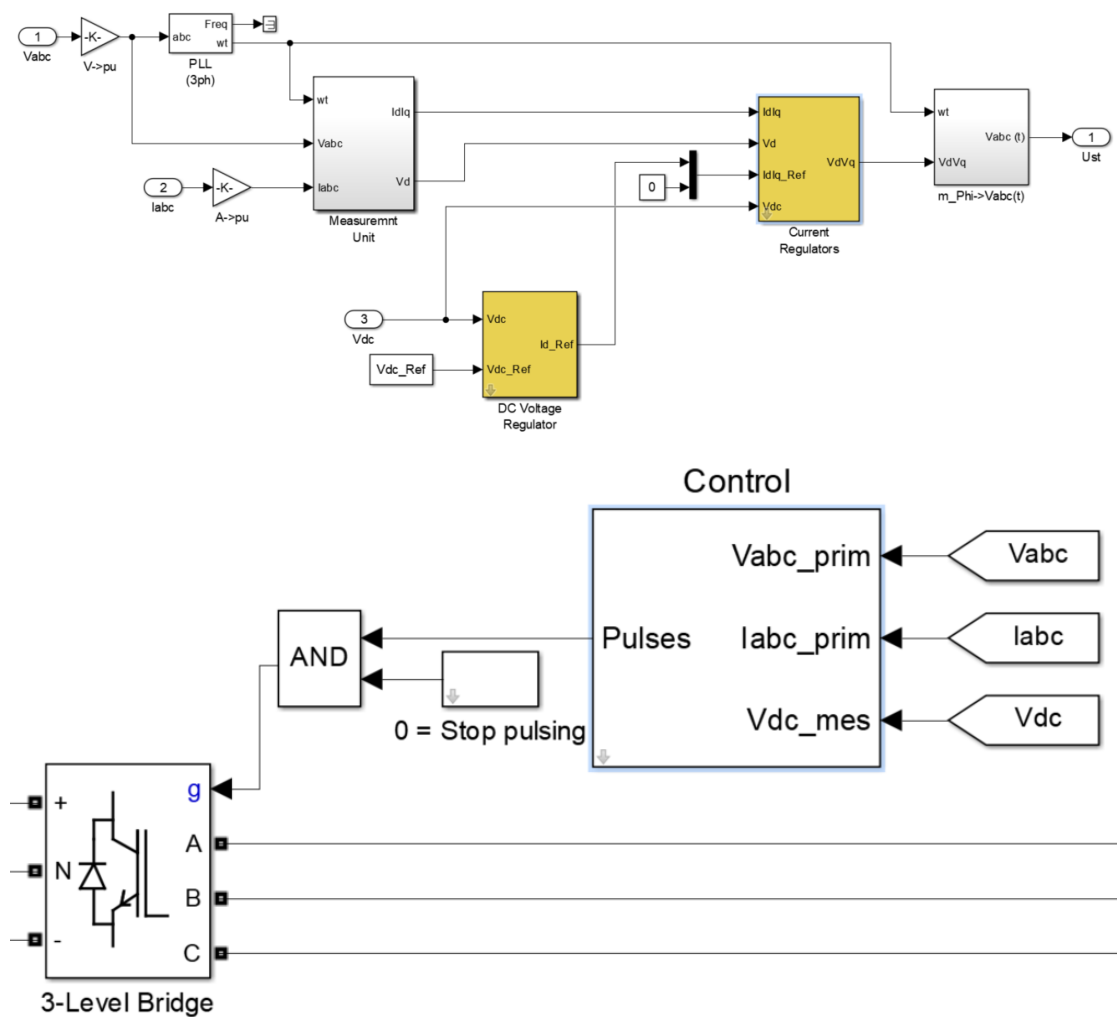


Fig.3.13 The simulation model of VSC inverter

The above two pictures are the simulation process of the VSC control system and the approximate structure diagram of the entire VSC inverter. We can use PWM from MPPT as the stop pulsing signal.

3.5 Grid

In the MATLAB command window, type powerlib command to open the power system module library. There are many module groups in the module library, mainly, it has Electrical sources, Elements, Power Electronics, Machines, Connectors, Measurements, Extras, Demos, Powergui, etc. Double click each icon can Open a module group.

The simulink model establishment mainly includes the following components: simplified generators, voltage-current measuring elements, transformers, transmission lines, loads, etc., set up a simulation model as shown.

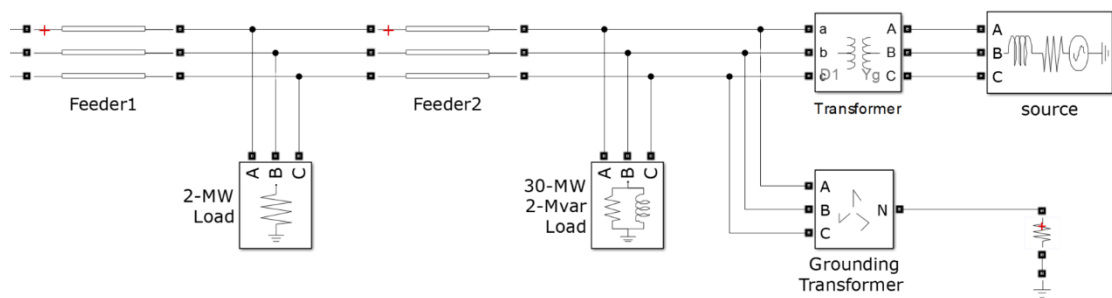


Fig.3.14 The simulation model of Grid

3.5.1 Measurements Component

Select the 3-phase V-I Measurements component from the library of measuring components, copy it and paste it into the circuit diagram.

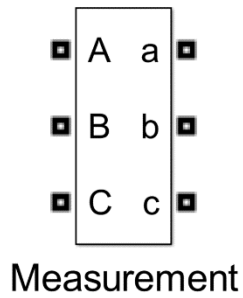


Fig.3.15 The 3-phase VI measurement component

Double-click the three-phase voltage-current measurement element and set the following in the three-phase voltage-current measurement element parameters dialog box: The voltage measurement options include three options, namely no-measure voltage (no) and phase-to-measure voltage (phase-to-phase). Ground) and measure the phase-to-phase voltage. There are options for measuring and not measuring current measurement options. In this example, the options for measuring phase voltage and measuring current are selected. Click the OK button to complete the parameter setting of the voltage-current measuring element.

3.5.2 Distributed Parameter Line

Select three-phase distributed parameter transmission line components from the line component library, copy and paste in the circuit diagram.

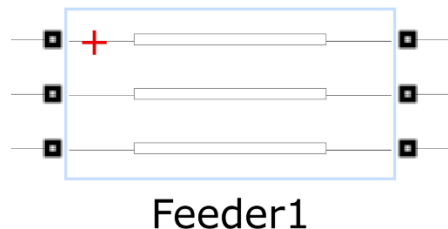


Fig.3.16 The 3-phase distributed parameter line component

Double-click the distribution parameter transmission line element and set it in the distribution parameter transmission element parameter dialog box. The parameter settings are as follows:

Table 3.1 The parameter setting of 3-phase distributed parameter line component

Number of phase N	3
Frequency for Resistance, Inductance, and Capacitance	50
Resistance per unit length	[0.01273 0.3846]
Inductance per unit length	[0.9337e-3 4.1264-3]
Capacitance per unit length	[12.74e-9 7.751e-9]
Line Length	300
Measurements	Choose not to measure electrical quantities

Click the OK button to complete the setting of the three-phase distribution parameter transmission line.

3.5.3 RLC Load Components

Select three-phase series RLC load components from the line component library, copy and paste in the circuit diagram.



Fig.3.17 The 3-phase RLC load component

Double-click the three-phase series RLC load component and set it in the Three-phase series RLC load component parameter dialog box. The three-phase series RLC load component parameter dialog box contains five options, namely the nominal phase voltage and the rated frequency, Three-phase active power (P), Three-phase Inductive reactive power (I), Three-phase capacitive reactive power (C) options.

Three-phase series RLC load element parameters are set as follows:

Table 3.2 The parameter setting of 3-phase RLC load component

Normal frequency	50
Three-phase active power (P)	50e6
Three-phase inductive reactive power (I)	0
Three-phase capacitive reactive power (C)	0

Click the OK button to complete the setting of the three-phase series RLC load element parameters

3.5.4 Three-phase Transformer Components

Select three-phase transformer components from the line component library, copy and paste in the circuit diagram.

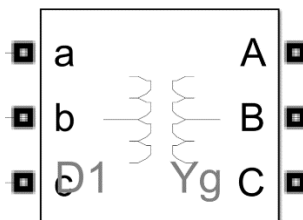


Fig.3.18 The 3-phase transformer component

Double-click the three-phase transformer component and set it in the Transformer Component Parameters dialog box. The Transformer Component Parameters dialog box contains the following options: Normal power and frequency; Winding1 connection; Winding parameters; Winding2 connection; Winding parameters; Magnetization resistance R_m ; Magnetic induction (Magnetization reactance L_m) and Measurements.

The transformer parameters are set as follows:

Table 3.3 The parameter setting of 3-phase distributed parameter line component

Normal power and frequency	[250e6 50]
Primary winding connection	Y
Primary winding parameters	[424.35e3, 0.002, 0.08]
Secondary winding connection	Delta
Secondary winding parameters	[315e3, 0.002, 0.08]
Magnetization resistance R_m	500
Magnetization reactance L_m	500
Measurements	Select Do Not Measure Options

Click the OK button to complete the setting of the three-phase transformer.

Chapter 4 Result

4.1 The Performance of PV Array

So far I completed the construction of the whole PV model. And the following step is to test the circuit voltage output and current output, which change with time.

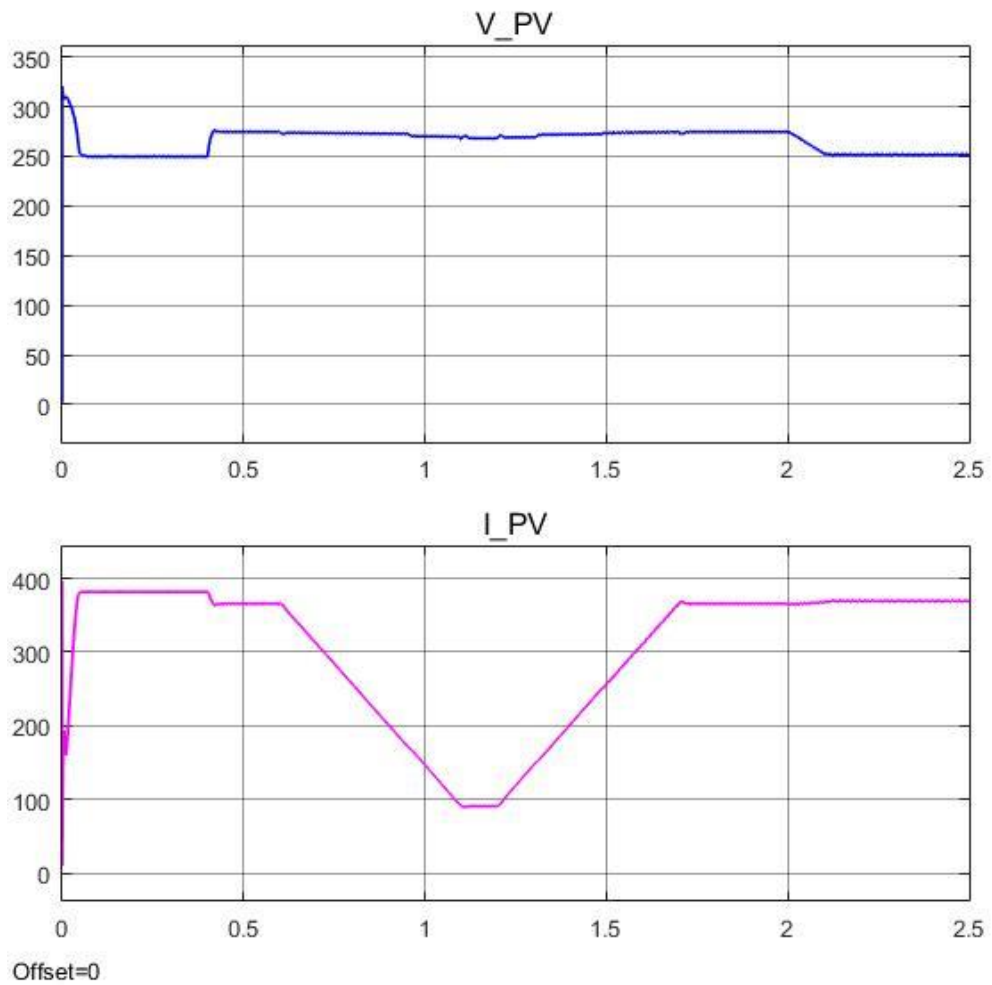


Fig.4.1 The voltage and current output of PV array

And we can also see the Volt-ampere characteristics and the peak power point as the temperature change from 25 to 50 from the figure 4.2:

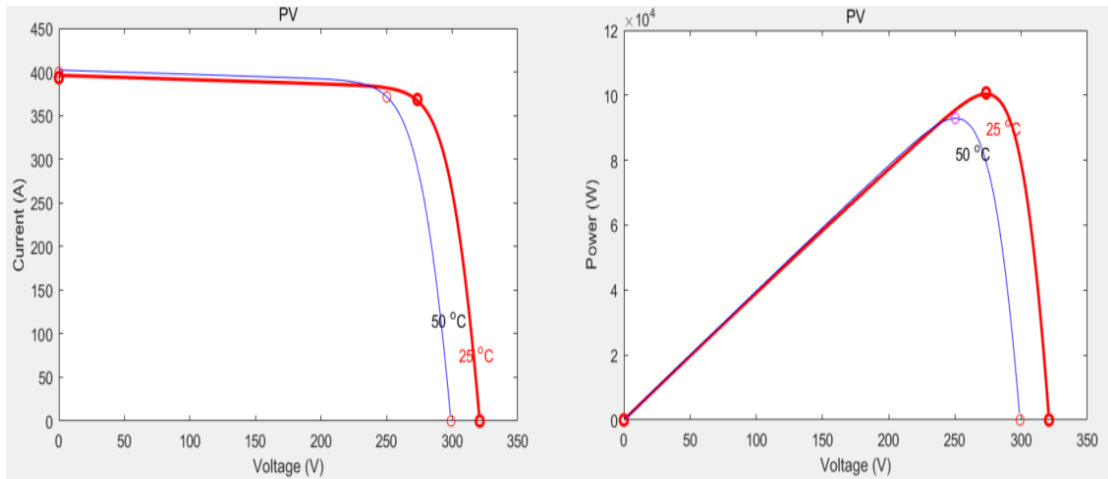


Fig.4.2 The characteristics of I-V and P-V at different temperature

After many tests after modifying the parameters, I found that the current will decrease with the increase of the voltage, and initially reduce the speed slowly, until the voltage value is close to 300V, the current drop rate increases suddenly. Also, there will be a peak in power as the voltage value changes, and the lower the temperature, the higher the peak power.

And finally, here we got the specific performance of this PV array:

Table 4.1 The performance of PV array

Power Density at STC (W / m2)	187.117
Power Density at PTC (W / m2)	172.147
Vmp: Voltage at Max Power (V)	54.7
Imp: Current at Max Power (A)	5.58
Voc: Open Circuit Voltage (V)	64.2
Isc: Short Circuit Current (A)	5.96
Cell Efficiency (%)	18.7%

After measurement, the output value of mean voltage is 251.65V, the mean power is 92.90kW, efficiency of this PV part is 18.7%.

4.2 The Performance of Boost Converter

And we can compare the voltage changes after using Boost Converter with MPPT function:

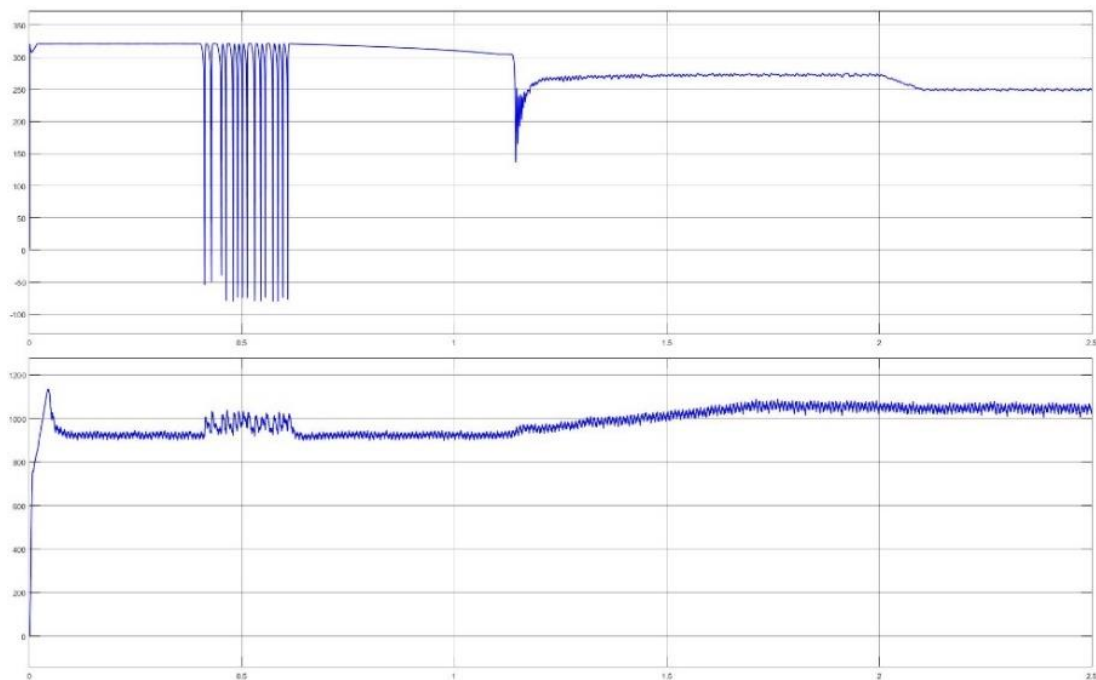


Fig.4.3 The change of voltage after using Boost Converter with MPPT

It can be seen in the figure 4.3 that the boost circuit reaches a steady state after about 2S, the output voltage is stable at 1050V, there will be a small oscillation, because the duty cycle of PWM output square wave is about 0.75, the photovoltaic cell output stable voltage is 250V, which consists the circuit boosting law ($U_o = 1 / (1 - \alpha) E$).

After measurement, the output value of voltage after the inverter is 499.99V, the mean power is 91.64kW, so we can get the efficiency is 98.6%.

4.3 The Performance of VSC Inverter

Next we will take a look at the simulation voltage waveform after using VSC inverter compare to the waveform from grid. We can see that they have the same frequency 60Hz because of the existence of PLL in VSC inverter, and all we need to do is to add a transformer to fit the magnitude of the voltage from the inverter.

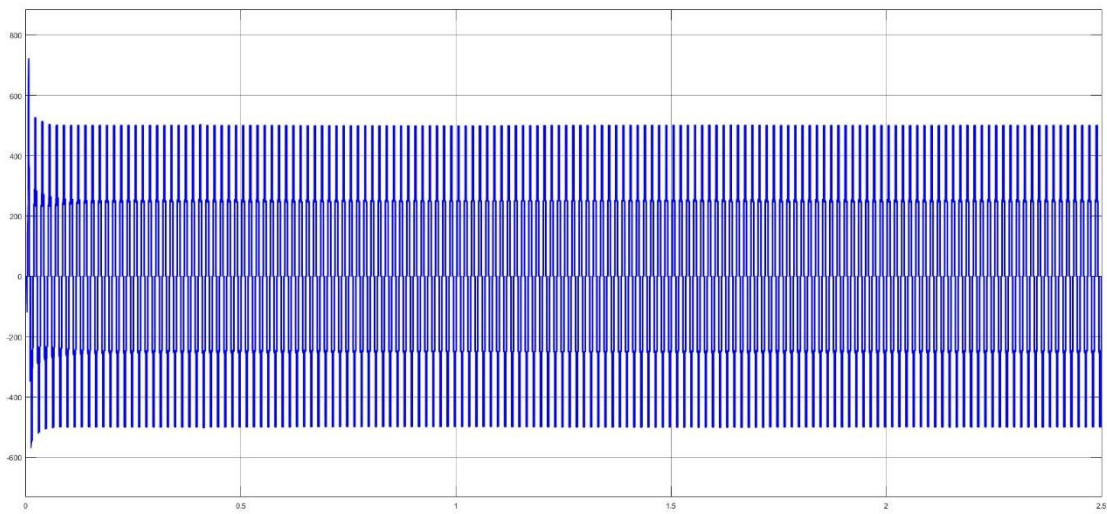


Fig.4.4 The voltage waveform after using VSC inverter

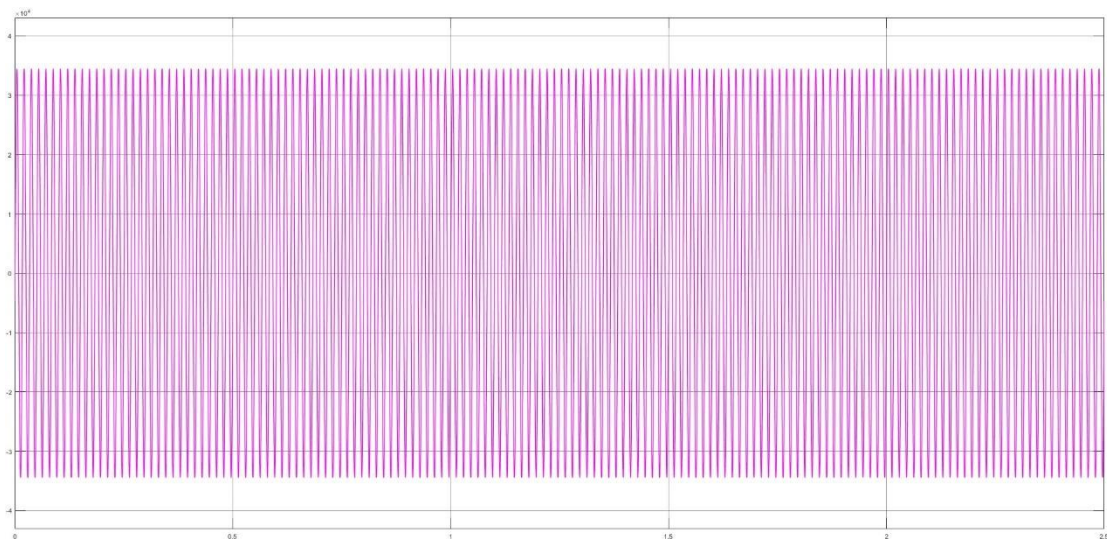


Fig.4.5 The voltage waveform of grid

After measurement, the output value of mean power after inverter is 91.27kW, so we can get the efficiency of the inverter, that is 99.5%.

4.4 Efficiency

So we can calculate the whole efficiency by multiply all the efficiency from the PV, boost converter, VSC inverter. But In the real industry, photovoltaic temperature factors need to be taken into consideration (photovoltaic cell efficiency will change with the temperature change during operation. When their temperature increases, the efficiency of crystalline silicon photovoltaic cells tends to decrease. Consider this loss. 2.5%), energy losses in photovoltaic power stations, such as line losses (energy loss in photovoltaic power plants, etc., taking into account the loss of approximately 2.5%), availability of the system (although the failure rate of photovoltaic modules is extremely low, but periodical overhaul and grid Failure will still cause damage. Take 2%).

Considering the above factors, the total power generation efficiency of the photovoltaic power station system is calculated and calculated as:

$$18.7\% * 98.6\% * 99.5\% * 97.5\% * 97.5\% * 98\% * 96.8\% = 16.5\%$$

Chapter 5 SUMMARY & CONCLUSION

5.1 Overview of the Project

This paper introduces the simulation model of the solar PV power station. First of all, we need to build a PV array based on the photovoltaic effect. In this project, the PV parameters I use are SunPower's SPR-305E-WHT-D. Here we need to simulate two sources of light radiation intensity and ambient temperature. Then in order to ensure accuracy, we simulated the diode as a controlled current source in Simulink, which is more convenient for calculation and measurement. Then in order to meet the industrial needs, the photovoltaic voltage needs to be boosted. In this project, I set a target voltage of 500V, so I used a DC-DC boost circuit. Of course, as explained in the results section above, it will also be accompanied by a certain amount of loss. At the same time, in order to ensure that the boost circuit works at the highest efficiency point, I use the MPPT method to use the error of the maximum power point as the duty cycle signal and generate the PWM wave as the switching signal of the boost circuit. Next, we need to convert the DC voltage into an AC voltage and integrate it into the grid. We need to get the voltage that is consistent with the frequency and phase of the grid. I chose to use a VSC three-phase inverter and use a PLL to meet the frequency and Phase.

Finally, the total efficiency of the simulated photovoltaic power plant is 16.5%, and the efficiency of the control system circuit is 88%, which is higher than the average system efficiency of 80%.

5.2 Improve Power Generation Efficiency

So what is the system efficiency of photovoltaic power plants? We can see the following table:[20]

Table 5.1 The system efficiency of PV station around the world

Age	Area	System Efficiency	Mean Efficiency
1980s	World	0.5~0.75	-
1990s	World	0.5~0.85	0.65~0.70
	Germany	0.38~0.88	0.67
2000s	France	0.52~0.96	0.76
	Belgium	0.52~0.93	0.78
	Germany	0.7~0.9	0.84

From this table, it can be seen that although the level of different countries will be different, but with the advancement of technology and the accumulation of experience, the efficiency of the photovoltaic power plant system is constantly improving worldwide.

The factors that affect the power generation efficiency of photovoltaic power plants are mainly divided into three categories: natural factors, equipment factors, and human factors. Although the temperature coefficient and solar radiation intensity have a great influence on the efficiency of photovoltaic cells, I think that equipment and human factors are the main factors that affect the generation rate. such as:

Photovoltaic module matching

Although the nominal parameters of the components are the same, the output characteristics are in fact different, which results in reduced efficiency due to inconsistent currents when multiple components are connected in series.

Inverter

Although the European efficiency in the inverter specifications considers the weighted conversion efficiency after different load ratios, in actual use, few inverters can reach 98.5% of the currently widely used. In the process of DC to AC in the inverter, the weighted efficiency of 97.5% should be good. The MPPT tracking effect of different inverters is also not the same. When the maximum power point voltage changes with the irradiance, the inverter needs to continuously change the voltage value to find the maximum power point voltage, which also results in energy loss due to the tracking hysteresis. At present, some inverter manufacturers use multiple MPPT methods to reduce this loss. In the range of maximum DC input voltage, as many series components as possible increase the voltage and reduce the current, which can improve the conversion efficiency of the inverter and reduce the line loss.

DC line loss, AC line loss

A 1MW unit has an area of about 3.5 to 4 hectares. To send electricity from such a large area photovoltaic module to a place requires a long DC line. There are two ways to reduce the line loss: use a good cable and increase the voltage.

Cleaning

The greater the irradiance, the stronger the penetration of sunlight and the less damage caused by dust. In addition to dust, if snow is not removed in time, it will cause a greater loss of power generation.

References

- [1]. U.S. Energy Information Administration, “Electric Power Monthly with data for June” , Independent statistics and analysis, 2016.
- [2]. Richard M. Swanson. Photovoltaics Power Up, Science, Vol. 324, 15 May 2009, p. 891.
- [3]. BaiduBaiké: Photovoltaic power generation, 2018.
- [4]. Bimal K. Bose. Energy, Environment, and Advances in Power, IEEE [J] . Trans. Power Electron, 2000(15) ; 688-701.
- [5]. R.C. Dugan and T.E. McDermott, “Distributed generation” IEEE Ind [J] .Appl. Mag., vol.8, no.2, pp.19-25, Mar./Apr.2002.
- [6]. DU Xiong, ZHOU Luowei, SHI Ying. VSC for renewable energy generation integration [J] . Electric Power Automation Equipment, 2009, 29 (8) : 100-105.
- [7]. REN Biying, ZHONG Yanru, SUN Xiangdong, et al. Simulation modeling of characteristics of PV cells based on PSIM software [J] . Journal of Xi’an University of Technology, 2007, 23 (4) : 257-260.
- [8]. HOHM D P, ROPP M E. Comparative study of maximum power point tracking algorithms using an experimental, programmable, maximum power point

tracking test bed [C] //28th IEEE Photovoltaic Specialists Conference.
Anchorage, AK, USA: IEEE, 2000: 1699-1702.

- [9]. SALAS V, OLIAS E, BARRADO A. Review of the maximum power point tracking algorithms for stand-alone photovoltaic systems [J] . Solar Energy Materials and Solar Cells, 2006, 98 (11) : 1555-1578.
- [10]. Prabakaran.K, Chitra.N, A.Senthil, “Power Quality Enhancement in Micro Grid- A Survey.” IEEE, ICCPCT-2013.
- [11]. M. Ebad and B. Song, "Improved Design and Control of Proportional Resonant Controller for Three-Phase Voltage Source Inverter," in IEEE Conference, 2012.
- [12]. A Yazdani and R Iravani, Voltage-Sourced Converters in Power Systems. New Jersey: John Wiley & Sons, Inc, 2010.
- [13]. Nikos Hatziargyriou ,”Microgrids-the Future of Small Grids”, Financial Planning Services, National Technical University of Athens, Greece ,2005.
- [14]. HERTEM V D, GHANDHARI M. Multi-terminal VSC HVDC for the European supergrid: obstacles [J]. Renewable and Sustainable Energy Reviews, 2010, 14(9): 3156-3163.
- [15]. BEERTEN J, COLE S, BELMANS R. Generalized steady-state VSC MTDC model for sequential AC/DC power flow algorithms[J]. IEEE Trans on Power Systems, 2012, 27(2): 821-829.

- [16]. ZIMMERMAN R D, MURILLO-SANCHEZ C E, THOMAS R J. MATPOWER: steady-state operations, planning, and analysis tools for power systems research and education [J]. IEEE Trans on Power Systems, 2011, 26(1): 12-19.
- [17]. Remus Teodorescu, Marco Liserre, Pedro Rodriguez, “Grid Converters for Photovoltaic and Wind Power Systems”, John Wiley and Sons, 2011.
- [18]. Tamas Kerekes, “Analysis and Modeling of Transformerless Photovoltaic Inverter Systems”, Department of Energy Technology , Aalborg University, 2009.
- [19]. Zhang Housheng; Zhao Yanlei; , "Research on a Novel Digital Photovoltaic Array Simulator," Intelligent Computation Technology and Automation (ICICTA), 2010 International Conference on , vol.2, no., pp.1077-1080, 11-12 May 2010.
- [20]. EPIA. Global market outlook for photovoltaics until 2019, 2014.